# Metal artifact removal
# In c-arm cone-beam ct

Group 4
Carolina Cay-Martinez, Marta Wells

## Report #4
## MAR application & Data Analysis

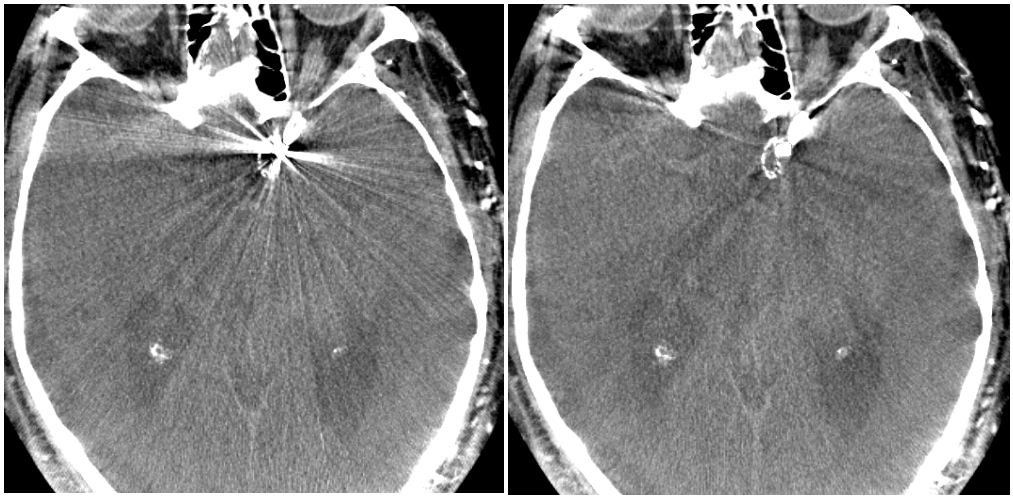

CT image of coil before and after MAR algorithm application
Image provided by Radvany, MD

The Johns Hopkins University
Advanced Computer Integrated Surgery

Project Advisors:
Jeffrey H. Siewerdsen, Ph.D.
Martin Radvany, MD (Interventional Radiology)
Tina Ehtiati, Ph.D. (Siemens Healthcare)

Metal artifacts introduce systematic discrepancies between the raw data values and the reconstructed image data values in computed tomographic (CT) reconstruction techniques. These discrepancies, which may include streaking artifacts, and visual obstruction of surrounding soft tissue, can seriously degrade the image quality and image fidelity of CT imaging in interventional radiology procedures. Metal artifact removal (MAR) algorithms have been developed and are ready for clinical testing. Prior to clinical trials with such MAR techniques, quantitative analysis of their performance is essential. Data analysis performed in this project will undertake such quantitative assessment of image quality and image fidelity by testing a recently developed MAR technique in an endovascular coiling and clipping intervention guided by CT imaging using custom phantoms designed to emulate the treatment of aortic aneurysms.

## I. Introduction

Artifacts arising from stents, coils and clips currently challenge C-arm cone-beam CT (CBCT) guidance of neurovascular interventions. Metal artifact removal algorithms (MAR) that diminish such artifacts for improved guidance and verification have been newly developed. To evaluate the performance of such algorithms, preclinical studies of an anthropomorphic head phantom emulating three endovascular interventions for the treatment of intracranial aneurysms were conducted using a robotic C-arm (Zeego, Siemens) for 3D CT imaging.

The primary purpose of medical imaging systems is to create accurate images of the internal structure and function of the body for diagnostic purposes or interventional treatment of diseases. The ability of medical professionals to successfully accomplish these tasks strongly depends on the fidelity of the images (the degree to which the image successfully represents the anatomy) and the quality of the images (the degree of degradation or distortion introduced into the image). Metal objects present in a CT image introduce metal artifacts, which are caused by *beam hardening*, *partial volume effects*, *photon starvation,* and *undersampling.* These artifacts result in heavy streaking patterns emanating from the metal object. Image quality assessments comprise the measurements of contrast, noise and artifact degradation while image fidelity assessments compromise the accuracy of the metal segmentation and the accurate anatomical representation of objects and surrounding soft tissue.

Post-acquisition processing of CT image data was performed on the dedicated Leonardo workstation (syngo, Siemens) using the syngo InSpace3D reconstruction algorithms. File formats for raw data (including relevant calibration files), reconstructed data and MAR corrected data were successfully obtained. Reconstruction was performed with the following parameters: XXXXX

The metal artifact removal algorithm used in the MAR application is a InSpace prototype version made available by Siemens Healthcare. The algorithm is based on work by Prell et. al.[1] The approach is based on a quasi-iterative, three-step correction scheme using a forward projection-based calculation of surrogate attenuation values for each single detector element for each projection with a dedicated segmentation process of the initial corrected image.

## II. Data Analysis for First Stage Phantom: Metal Spheres

### MAR Algorithm Application

It was found that after the first image acquisition of 02/28/2013???? the Zeego C-arm was un-calibrated. This produced unwanted geometric artifacts in the images obtained, hindering further data analysis. After C-arm calibration, a new calibration file was obtained and images were reconstructed again. Geometric artifacts were corrected with the acquisition of the new files.

- Include MATLAB generated picture of geometric artifact affected image.

---

[1] Prell, et. al. "A novel forward-projection based metal artifact reduction method for flat-detector computed tomography" 2009 *Phys. Med. Biol.* **54** 6575

Discuss problem with algorithm and licensing. An update to the licensing needed to be completed before further application. Various algorithm-error log files were sent to Siemens

## Methods

The magnitude of the artifact in each image was calculated as the average standard deviation in each vertical plane in the region directly surrounding the metal sphere, but not including the sphere itself.

1. For the smallest size metal spheres, 3.2mm, locate the center point coordinates of the sphere in the image.
    a. Select a rectangular box ROI (see Figure 1) of 5x5x4 pixels around this center point to represent the sphere area.
    b. For the background ROI, select the area that is enclosed by the region between two concentric circles of radii 10 and 30 pixels around the center point for each sphere. The left half of this combined region in the four z-planes of interest forms the background ROI of a semicircular annulus.
2) For the middle size metal spheres, 6.4mm, locate the center point coordinates of the sphere in the image.
    a. Select a rectangular box ROI of 9x9x8 pixels around this center point to represent the sphere area.
    b. For the background ROI, select the area that is enclosed by the region between two concentric circles of radii 15 and 32 pixels around the center point for each sphere. The left half of this combined region in the eight z-planes of interest forms the background ROI of a semicircular annulus. This selection ensures that the inner circle of the annulus is proportionally the same distance away from the center of the sphere as in the background ROI in the images with the smallest spheres, and that the total area enclosed in the ROI for both sizes of sphere is the same.
3) For the largest size metal spheres, 12.8mm, locate the center point coordinates of the sphere in the image.
    a. Select a rectangular box ROI of 15x15x16 pixels around this center point to represent the sphere area.
    b. For the background ROI, select the area that is enclosed by the region between two concentric circles of radii 25 and 38 pixels around the center point for each sphere. The left half of this combined region in the sixteen z-planes of interest forms the background ROI of a semicircular annulus. This selection ensures that the inner circle of the annulus is proportionally the same distance away from the center of the sphere as in the background ROI in the images with the smallest and medium spheres, and that the total area enclosed in the ROI for all sizes of sphere is the same.
    c. Note: The 12.8mm tungsten sphere had detached from its insertion rod earlier in the procedure, so we were unable to image it near the clivus, as with the other spheres.
4) In each of these two ROIs, the sphere and background regions, measure the mean ($\mu_{sphere}$ and $\mu_{background}$), and standard deviation ($\sigma_{sphere}$ and $\sigma_{background}$ ) of the attenuation in both the original CT reconstruction images and the corresponding MAR corrected images.
5) Calculate $CNR = \frac{C}{\sigma} = \frac{|\mu_{sphere} - \mu_{background}|}{\sigma_{background}}$ for both the original and MAR corrected images.

## Results

## Image Quality and MAR Algorithm Analysis

High CNR values = better image quality. Data shows that CNR increases after MAR correction.

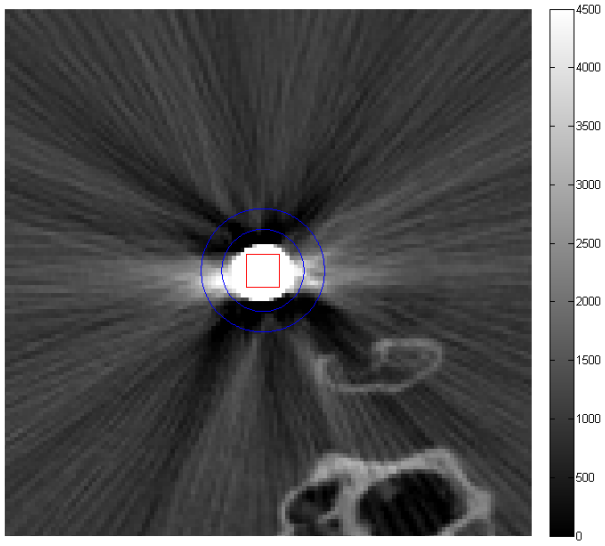


****measure CNR of plastic spheres

In order to analyze the distortion created by the metal artifact,

Extra notes:
Mar affecting any other objects
Set standard greyscale for all images, add colorbar to see range
Window – min to max contrast, level – center of window
otes : v

Table 1: Relevant values in images without MAR application

| **Metal** | $\mu_{sphere}$ | $\sigma_{sphere}$ | $\mu_{ROI}$ | $\sigma_{ROI}$ |
|---|---|---|---|---|
| 3.2mm, titanium | | | | |
| 3.2mm, steel | | | | |
| 6.4mm, steel | | | | |
| 3.2mm, tungsten | | | | |
| 6.4mm, tungsten | | | | |